

## 6. *Water Level Oscillations on the Continental Shelf in the Vicinity of Miyagi-Enoshima.*

By Isamu AIDA,

Earthquake Research Institute.

(Read Sept. 27, 1966.—Received Dec. 28, 1966.)

### Abstract

The spectra of tsunamis observed on a continental shelf are closely related to the spectra of water level fluctuations in ordinary days with the period of 10 to 100 minutes, the so-called back-ground spectra. Therefore, the nature of back-ground oscillations on the shelf in the vicinity of Enoshima Island, Miyagi Prefecture, where a tsunami observatory is located, has been investigated. Theoretical trapped and leaky modes of oscillations were computed for the shelf near Miyagi-Enoshima and also the records of the back-ground oscillations sampled from the data through the year in 1965 were examined by means of the Fourier analysis. The Fourier spectrum averaged through a year coincided fairly well with the theoretical spectrum of the leaky mode for the constant spectral input offshore, particularly in the period band shorter than about 40 minutes. In the periods longer than about 50 minutes, the spectral intensity of the back-ground is much larger than the theoretical spectrum. There is a possibility that the incoming waves which excite back-ground oscillations may be more intensive in the longer period band. Another possibility is the contribution of the trapped waves for this period band. Very often the phase delay time obtained from the phase angle of the Fourier spectrum coincides fairly well with the one derived from the calculated dispersion curve on the assumption that waves start from a localized source with the same phase for all frequency. This suggests the existence of edge waves. However, the coherency analysis of water level variations observed simultaneously at Enoshima and Ōfunato, contains an obscurity on the existence of waves propagating along the shelf.

### 1. Introduction

Several years ago, the spectral analysis of long-period ocean waves including several tsunamis was carried out by R. Takahasi and the

author<sup>1)</sup> for the records obtained at the Enoshima Tsunami Observatory, attached to the Earthquake Research Institute, University of Tokyo. And it was shown that the peaks in spectra of tsunamis coincided well with the ones for water level fluctuations in ordinary days, the so-called back-ground spectra. Furthermore, the amplitudes of tsunami spectra accompanying large earthquakes were large in the longer period part of the back-ground spectrum, those for small earthquakes being large in the shorter period part. Therefore, it can be said that the character of water level fluctuations on the shelf is an important factor in deciding the behavior of tsunami waves in this area.

On the other hand, the existence of edge waves was suggested by W. Munk and F. Snodgrass et al<sup>2)</sup> on the basis of dispersive wave trains observed at the time of passing of a hurricane along the continental shelf and later they<sup>3,4)</sup> investigated back-ground spectra over California's continental borderland, and concluded that most part of energy of the long-period water level fluctuations was in the so-called trapped mode. The dispersive waves of tsunamis, which were supposedly edge waves, were also investigated in the cases of Iturup tsunamis in 1958 and 1963.<sup>5)</sup>

The investigations on the long-period ocean waves over a continental shelf have been made from various view-points as mentioned above. In the present study, the author investigates the nature of the long-period water level fluctuations on the shelf in the vicinity of Enoshima Island, Miyagi Prefecture, in ordinary days. First, the trapped and leaky modes of shelf oscillations will be calculated for the actual depth profile obtained from the bathymetric chart. Next, the behaviour of the actual shelf oscillations will be examined by means of the Fourier analyses for the records observed at Miyagi-Enoshima. The Enoshima Tsunami Observatory has been performing a routine observation of long period ocean waves since 1956. Therefore, the records of water level fluctuations can be obtained all the year round. If a seasonal change in the nature of these fluctuations exists, it will be found by analyzing the

1) R. TAKAHASI and I. AIDA, "Studies on the Spectrum of Tsunami," *Bull. Earthq. Res. Inst.*, **39** (1961), 523, (in Japanese).

2) W. MUNK, F. SNODGRASS and G. CARRIER, "Edge waves on the continental shelf," *Science*, **123** (1956), 127.

3) F. SNODGRASS, W. MUNK and G. MILLER, "Long-period waves over California's borderland, Part I," *Jour. Mar. Res.*, **20** (1962), 3.

4) W. MUNK, F. SNODGRASS and F. GILBERT, "Long-waves on the continental shelf," *Jour. Fluid Mech.*, **20** (1964), 529.

5) T. HATORI and R. TAKAHASI, "On the Iturup Tsunami of Oct. 13, 1963, as observed along the Coast of Japan," *Bull. Earthq. Res. Inst.*, **42** (1964), 543.

records during the year round. In the following chapters, the author will show the results of theoretical calculations and analyses of actual records, and will try to interpret the observational facts in the light of the theoretical expectation.

## 2. Results of the mode computation

The Pacific coast in the northeast of Japan, where tsunamis occur frequently, is taken for the area of this problem. As shown in Fig. 1, the profile *a* is offshore of Miyagi-Enoshima, along the latitude  $38.5^{\circ}\text{N}$ , and profile *b* offshore of Ōfunato, along the latitude  $39.0^{\circ}\text{N}$ . Cross-sections of the shelf are shown in Fig. 2, these depth profiles being approximated by a series of 30 steps as shown by the fine line in the figure, provided the many steps in shallow water are omitted for simplicity of the drawing. The profiles are taken as far as the deep ocean basin, because all possible modes must be determined. In the computation, it is assumed that the depth profile does not change along the straight coast. Following W. Munk et al.<sup>6)</sup>, the wave equations are solved for each step with constant depth and their solutions patched by requiring continuity in the flux of mass and momentum across the step (See Appendix).

The computation is first carried out for the trapped modes, the calculated results being shown in Figs. 3 and 4 for the profiles *a* and *b* respectively, where the spatial frequency  $n$ , measured along the coast, is taken in cycle per km on the abscissa, and the time frequency  $f$  in cycle per hour on the ordinate. The straight line drawn obliquely

6) *loc. cit.*, 4).

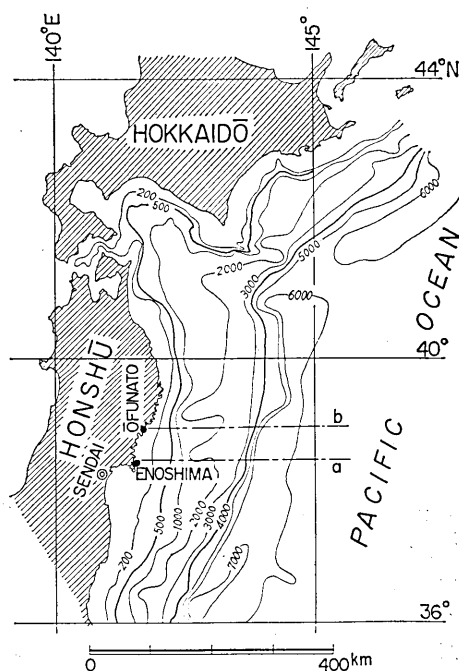


Fig. 1. Continental shelf off the northeast of Japan showing the station, Miyagi-Enoshima. The profiles along *a* and *b* are shown in Fig. 2.

through the origin shows the relation,  $f=c_N n$ , where  $c_N$  is the long wave velocity determined from the depth of the last step, namely the depth of deep water outside of the shelf. The line  $f=c_N n$  is a cut-off line the trapped waves existing only to the right of it, as shown with  $f(n)$  curves in the figures. The  $f(n)$  curves are labelled with the mode numbers 0, I, ... IV. In this domain, waves are allowed to exist only on these  $f(n)$  curves, therefore the spectrum is discrete. In Fig. 4, the curves shown by the broken lines are the ones of the 0th mode and the 1st mode

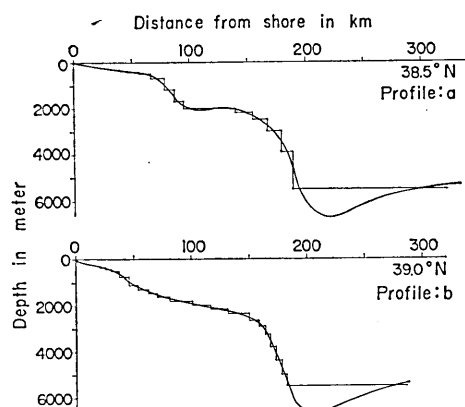


Fig. 2. Depth profiles along the lines  $a$  and  $b$  indicated in Fig. 1. The calculated profiles has been approximated by a series of 30 steps as shown by a fine line. The steps in the region of shallow water are omitted for simplicity of the drawing.

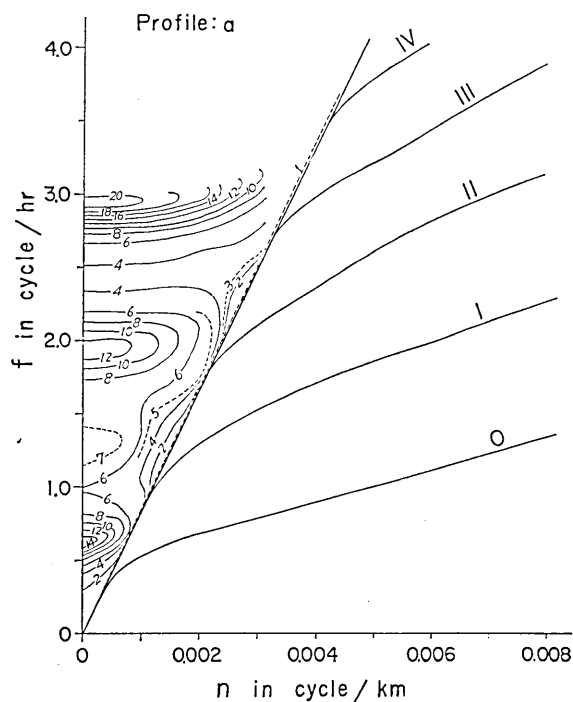


Fig. 3. Computed  $(f, n)$  diagram for profile  $a$ . The curves which are labelled with the mode numbers 0, I, ... IV show trapped modes. Leaky modes appear in the left side of the cut-off line drawn obliquely through the origin. Contours show the squared ratios of coastal to incident amplitude.

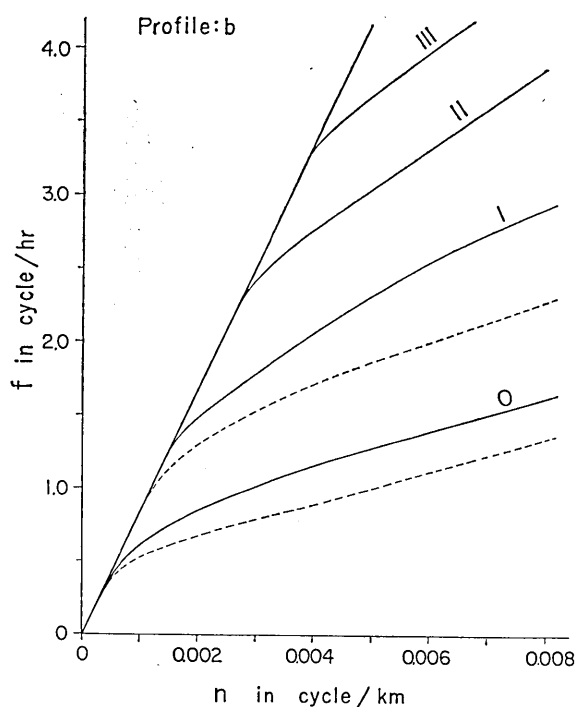


Fig. 4. Computed  $(f, n)$  diagram for the profile  $b$ , only trapped modes were calculated. The broken lines show the ones for the profile  $a$ , reproduced from Fig. 3.

for the profile  $a$  reproduced from Fig. 3. Comparing the curves for the profile  $a$  with those for the profile  $b$ , it is seen that they vary significantly according to the adopted bottom profile, particularly at the high frequency band and for higher modes. Accordingly, in the discussion of the wave propagation along the actual continental shelf, it may not be justified to assume the same profile of a shelf along the coast. However, as long as the long period part is concerned, the above assumption may be permissible as a first approximation.

Certain features of the  $(f, n)$  diagram deserve consideration. The slope,  $df/dn$ , of the discrete modes is the group velocity, and the slope,  $f/n$ , of the chord is the phase velocity. For both profiles  $a$  and  $b$ , the phase velocity  $V$  and the group velocity  $U$  are calculated as shown in Fig. 5. The suffix 0 on  $V$  or  $U$  indicates the 0th (fundamental) mode and the suffix I the 1st mode. When the waves caused by some disturbances are propagated along the shelf as trapped waves (edge waves),

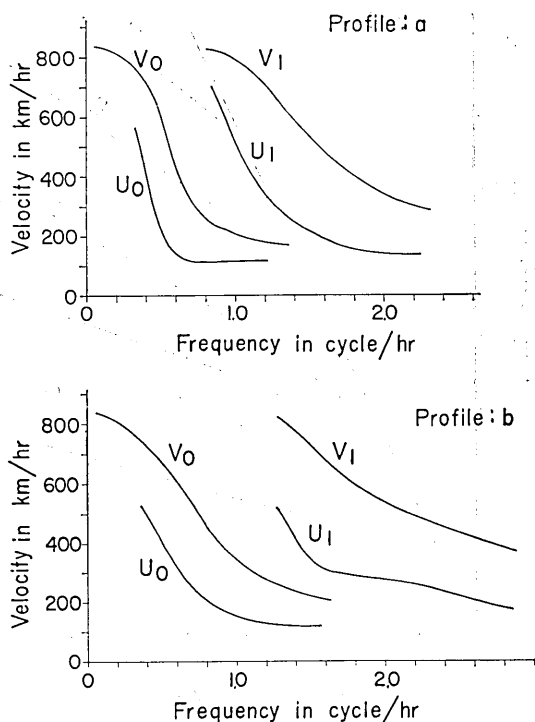


Fig. 5. Computed dispersion curves for trapped waves propagating along the shelf with the profile *a* and *b*. The curve labelled *V* indicates the phase velocity and *U* the group velocity. The suffixes 0 and 1 indicate the 0th and the 1st modes.

the waves will exhibit a dispersive feature. Since, the dispersion curves for profiles *a* and *b* only 55 km apart along the coast differ considerably, it might be necessary to take the longshore variation of the shelf profile into consideration when the observed waves are investigated with respect to edge wave modes.

The computation of the leaky modes is also carried out only for the profile *a*, the calculated results being shown again in Fig. 3. In the domain to the left of the cut-off line, there exist leaky modes, the spectra of which are continuous. The contour lines drawn in this domain display the squared values of ratios of coastal over incident amplitude,  $R(f, n)$ , as given by the equation (11) in Appendix. The values on ordinate correspond to ones in the case when the incident angle of waves is normal to the coast, and the cut-off line shows the case of glancing

incidence. The essential features are not changed as the incident angle of waves deviates somewhat from normal. But, near the glancing incidence, there is a domain between the cut-off line and the broken line shown by  $R=1$ , where the coastal amplitude is always less than the incident amplitude. The  $R(f)$  curve in the case of normal incidence has the maxima at the frequencies 0.62, 1.28, 1.96, 2.94, 3.76 and 4.35 cycle per hour as shown in Fig. 6, the sharpness of these peaks reflecting the radiational losses of wave energy from the shelf.

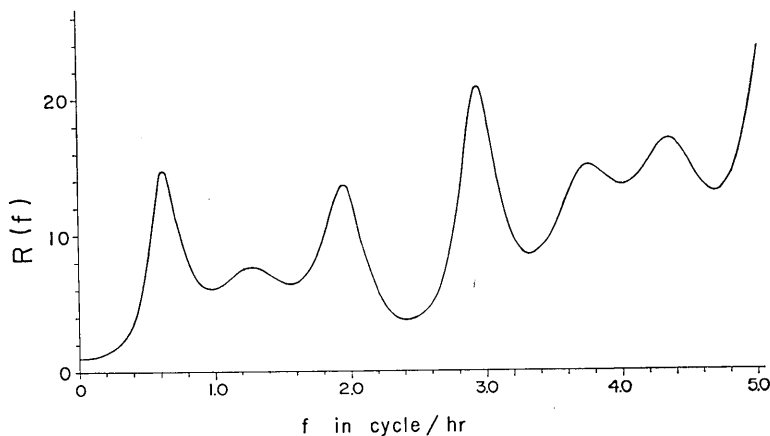


Fig. 6. Computed spectrum at shore for the leaky mode in the case of normal incidence.

The observed spectrum of waves at Enoshima, however, cannot be compared immediately with this  $R(f)$ , because Enoshima lies at a distance of several kilometers from the open coast and also the effect of Onagawa bay extending inland from the open coast cannot be neglected. Therefore, the effect of Onagawa bay is taken into account by means of a simplified model, namely, the problem is treated as a one-dimensional one. Onagawa bay is divided into twelve sections and the outer sea is treated as a channel with variable depth but with constant width. The estimation of the equivalent width of the channel is a complicated matter. Taking the discussion of K. Kajiura<sup>7)</sup> into account, the width of the hypothetical channel outward from Enoshima is assumed to be two times the one at the mouth of Onagawa bay. Inspecting a bathymetric chart, it is as-

7) K. KAJIURA, "Effects of a Breakwater on the Oscillations of Bay Water," *Bull. Earthq. Res. Inst.*, **41** (1963), 403, (in Japanese).

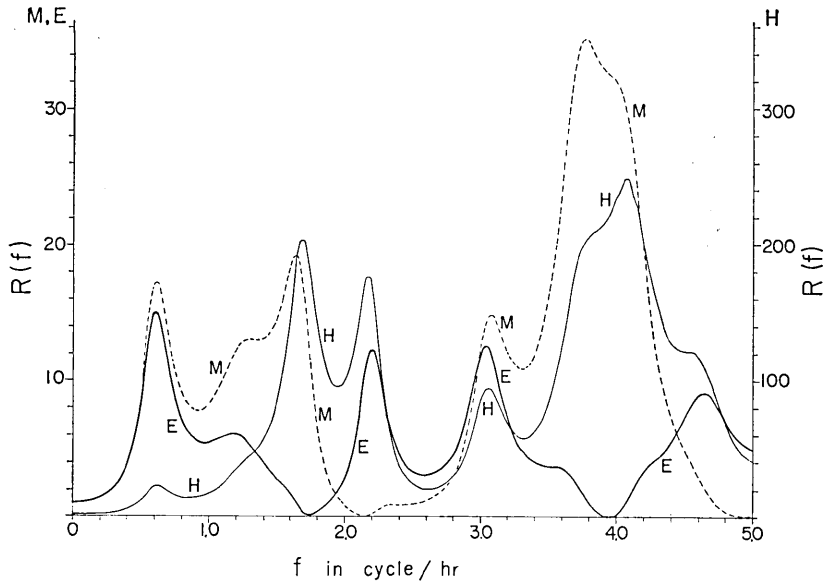


Fig. 7. Computed spectrum taking the effect of Onagawa bay into account. The labels E, M and H indicate the curves at Enoshima, the mouth and the head of Onagawa bay, respectively.

sumed that the width of the channel from the mouth of the bay to Enoshima spreads according to a quadratic curve. The result of the computation under these assumptions is shown in Fig. 7. In this figure, the curve labelled H shows the squared ratio of the bay head over incident amplitude, and the curve labelled M and E shows similar values at the mouth of the bay and at Enoshima, respectively. Now, as for the E curve, the first peak scarcely changes as compared with the former case without a bay (Fig. 6), but conspicuous valleys newly appear at frequencies of 1.74 and 3.95 cycle per hour (periods of 34.5 and 15.2 min), which are caused by the resonance of Onagawa bay. The essential factor deciding the behaviour of  $R(f)$  at high frequency parts is the topography near shore, so that a very different appearance of the spectrum results between Figs. 6 and 7 in the frequency band higher than 1.2 cycle per hour.

### 3. Analyses of the actual records

At the Enoshima Tsunami Observatory, a routine observation of long-



period ocean waves has been carried out using the two kinds of long-period wave recorders, the ERI-IV type<sup>8)</sup> and the Van Dorn type<sup>9)</sup>. Water level fluctuations of small amplitude (less than 3 cm) with various periods, so-called back-ground fluctuations, are always observed on the record even at the ordinary time, when there is no source of notable weather disturbance in the area. The records of such back-ground fluctuations observed by the Van Dorn type recorder were analyzed for one year in 1965. The segments of records for 24 hours on the 1st and 15th day of each month are chosen as representative samples. When the records on these days were highly disturbed by some causes, the one on the previous or following day was chosen as the substitute. A total of 24 records for 24 hours was read out with an interval of 2 minutes, their values being punched digitally on the IBM card in order to be analyzed by a digital computer. To attenuate the residual component of tide which remains after the hydraulic filtering of the recorder, the digital filter is applied by means of the subtraction of the values obtained by the running mean for 240 minutes. For filtered data, the spectral amplitudes and phases were calculated by means of the Fourier transform. Thus, we obtained 24 spectra of the back-ground fluctuations covering one year. The intensity of each spectrum varies considerably. One of the reasons is that the statistical deviation is expected to be large because of the insufficient length of the analyzed record. Another reason is that an essential deviation from spectrum to spectrum is expected when the spectrum of incoming wave changes. The scattering of the deviation of 24 individual amplitudes from the mean for each frequency band cannot be expressed by a normal distribution. However, for rough estimation of the deviation, the ratios of the standard deviations over the mean value are calculated. Ratios range between 0.4 to 0.7 and are rather large.

To investigate features of back-ground fluctuations, the averaged spectrum during a year is considered in two ways as follows:—

1) The 24 spectra, corrected for the frequency response of the long-period wave recorder, were averaged with respect to the spectral amplitude. Such averaged spectrum is shown in the upper part of Fig. 8. The peaks of the spectrum appear at the periods 96, 75, 58, 43, 28, 20

8) I. AIDA, "Design and Construction of Long-period Wave Recorders," *Bull. Earthq. Res. Inst.*, 40 (1962), 545, (in Japanese).

9) R. TAKAHASI, et al., "Observations at Miyagi-Enoshima Tsunami Observatory during the IGY Period," *Bull. Earthq. Res. Inst.*, 39 (1961), 491.

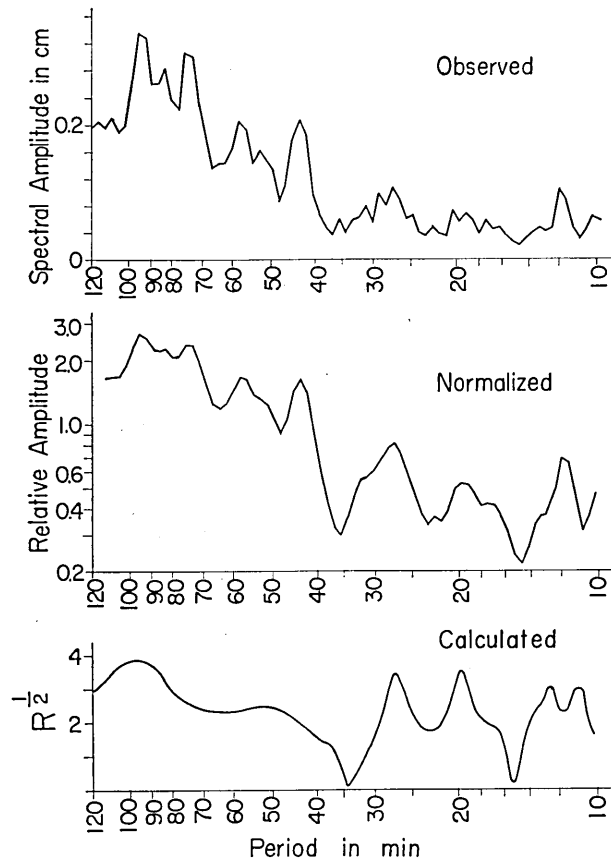


Fig. 8. Spectra of the back-ground fluctuations at Miyagi-Enoshima.  
 upper: Analyses of the record sampled 24 hours per 15 days were made through a year in 1965, and the 24 spectra obtained were averaged without any operation.  
 middle: Spectra were first normalized with respect to the mean amplitude of each spectrum, and were smoothed by means of the weighted running mean. The 24 spectra thus obtained were averaged.  
 lower: Computed spectrum obtained in the preceding chapter, in Fig. 7.

and 12 minutes, these periods coinciding well with what the author once obtained from the analysis of record for several days<sup>10)</sup>. The averaging process in this case was carried out without regard to the fluctu-

10) *loc. cit.*, 1).

ation of total energy level.

2) Since the total energy of each spectrum varies considerably, so-called normalizing was performed on all spectra, which was the procedure determining the relative spectral amplitude referred to in the mean level of each spectrum. These normalized spectra were smoothed by means of the weighted running mean for 3 values, in which a central value has the weight 2 and values on both sides the weight 1. The 24 spectra, normalized and smoothed, were averaged again. The result is presented in the middle figure of Fig. 8. In this case, the ratios of the standard deviations over the mean value are near by 0.3.

The features of the spectra, averaged in two different ways, do not differ essentially, but the latter spectrum is more readily visualized. The peak values for the longer period part over 70 minutes in the spectrum are about 3 times larger than the ones for the shorter period part under 30 minutes. Such a fact was also noticed by W. Munk et al.<sup>11)</sup>, who stated that the power spectral density at the frequency below 0.7 cycle per hour was proportional to  $f^{-3}$ . In the present case, the increase in the spectral amplitude at the longer period part is about  $f^{-1}$ , or equivalently  $f^{-2}$  in terms of the power amplitude.

In order to compare with these observational spectra, the calculated amplitude ratio of coastal over incident wave for the case of normal incidence obtained in the preceding chapter (the curve E in Fig. 7) is reproduced in the lowest part in Fig. 8. These observational and theoretical results show a striking coincidence, namely, the periods of maxima and minima in these spectra are exactly equal, especially in the period band less than 40 minutes. Namely, the back-ground spectrum at Enoshima can be explained fairly well by the leaky modes for the normal incidence, taking the effect of Onagawa bay into account. This fact tells us the following remarkable thing. Even if the observing station is located at some distance outward from a bay mouth, the observed water level fluctuations are affected considerably by the oscillations of bay water.

To examine the seasonal pattern of the back-ground spectra, the normalized spectra are averaged for 4 groups separately: Jan.—March, April—June, July—Sept., Oct.—Dec.. As shown in Fig. 9, these spectra being similar to each other, but the periods of peaks in the longer period part show the slight tendency to become longer in autumn and

11) *loc. cit.*, 3).

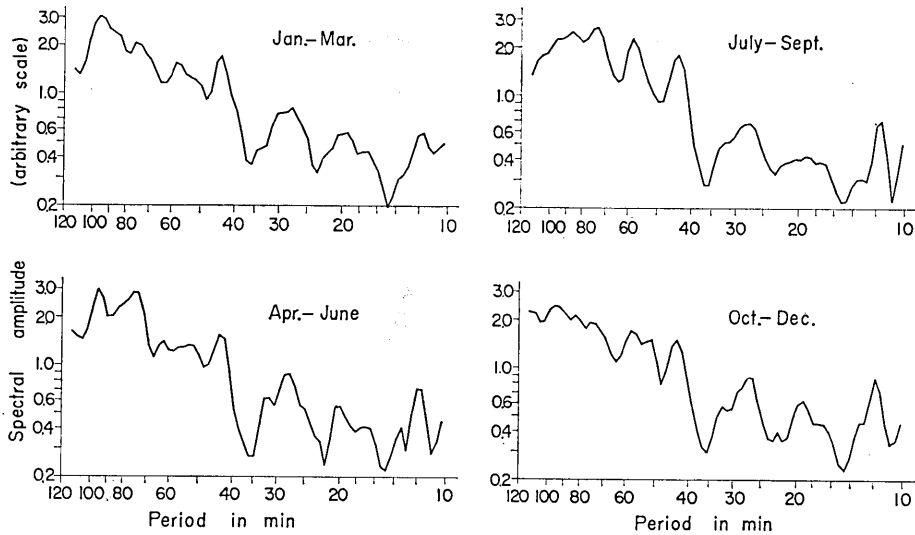


Fig. 9. Observed spectra for 4 seasons.

in winter. However, on the whole, it may be safe to say that the averaged spectra of back-ground do not change throughout the four seasons of a year.

It may be noticed that in the observed spectrum, the amplitude in the longer period part is considerably larger than that in the shorter period part. This fact may be interpreted in two ways. The one being that the incident wave energy density exciting the shelf oscillations is larger at the long period part than the energy density at the short period part. Another possibility is the dominance of the trapped mode waves in the long period part. According to the calculation in the preceding chapter, the behaviour of the trapped waves of higher modes and short periods depend severely on the profile of the shelf, but if the fundamental mode with long period only is considered, some restricted discussions may be possible, even if the shelf profile varies along the coast.

Assume that edge waves are generated at a point on a shelf at the time  $t_0$ , with the phase angle  $\beta(f)$ . Then the waves observed at a point separated by  $\Delta$  from the generating point must be delayed in the phase angle by

$$\theta(f) = 2\pi f \left( t_0 + \frac{\Delta}{V(f)} \right) - \beta(f),$$

where  $V(f)$  is the phase velocity of the edge wave. If there are many observation points on the shelf,  $t_0$ ,  $\Delta$  and  $\beta(f)$  can be determined by the phase angles of Fourier spectra of edge wave records at those points. In the present study, the observation was carried out only at one station, Miyagi-Enoshima, so the perfect solution cannot be obtained. Therefore, tentatively  $\beta(f)$  is neglected and also the phase characteristics of the recorder are left out of consideration, as they hardly change in the frequency range in question. Under these assumptions, the values of the phase delay time,  $\theta(f)/2\pi f$ , are calculated as the function of  $f$  from the Fourier spectra observed at Enoshima. On the other hand, the values,  $\Delta/V(f)$ , are calculated from the theoretical phase velocity shown in Fig. 5, with  $\Delta$  as a parameter. Comparing the observed and theoretical phase delay time, we could choose the parameter  $\Delta$  for the best fit of two curves as shown in Fig. 10. The left figure shows ex-

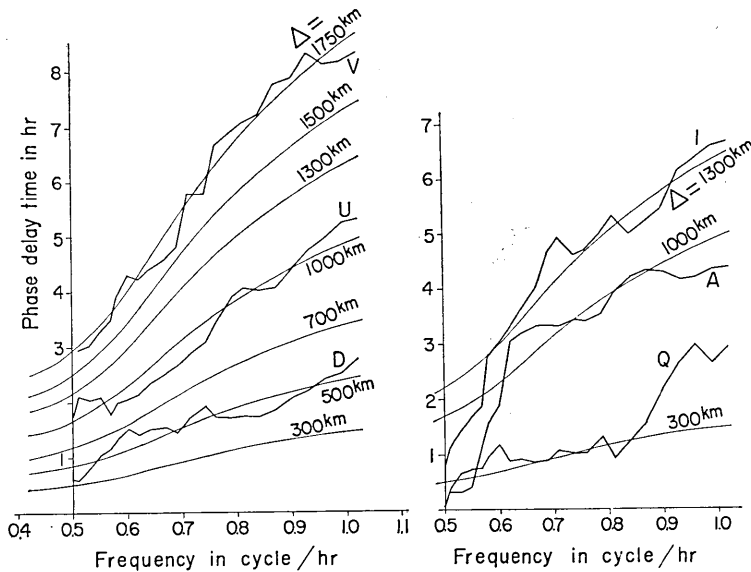


Fig. 10. Phase delay time of the spectra of back-ground fluctuations and one expected from the theory in the preceding chapter. Fine lines indicate the theoretical one for the propagating distance  $\Delta$ , and the thick lines are based on the observational values obtained from the spectral analyses of the record on the day labelled as shown below.

A: Jan. 1, 1965.  
D: Feb. 15, 1965.  
I: April 29, 1965.

Q: Aug. 31, 1965.  
U: Nov. 2, 1965.  
V: Nov. 15, 1965.

amples when the observational curve (thick line) coincides pretty well with the calculated one (fine line), and the right figure shows examples when they do not coincide. In the cases shown in the left figure, notable low atmospheric pressure regions were found over the shelf from Hokkaidō to the Kuril Islands during these periods according to the weather chart. Although the existence of trapped waves cannot be proved sufficiently with these examples, it may suggest the propagation of edge waves.

The observations at two stations at least are required for the solution of this problem on a more reliable basis. For this purpose, the record obtained at the mouth of Ōfunato bay on December, 1965<sup>12)</sup> is used. By combining this record with the one obtained at Enoshima during the same period, the power-spectra, the co-spectrum, the quadrature-spectrum, the coherence and the phase are calculated by Tukey's method as shown in Fig. 11. Records were read out with 2 minutes interval for 44.5 hours from just noon of the 5th of December. The characteristics of the recorders used at Ōfunato and Enoshima were

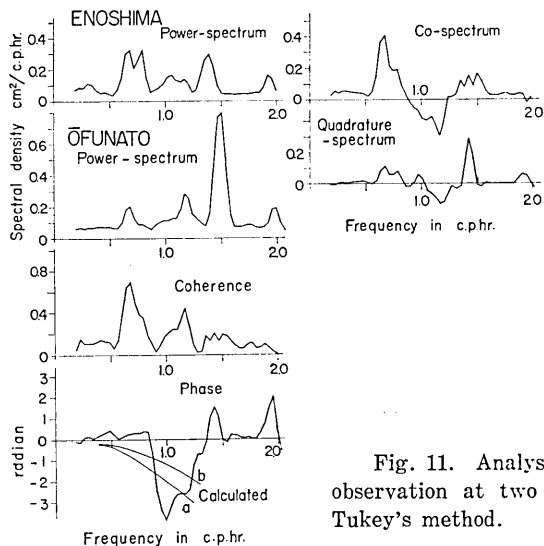


Fig. 11. Analysis of the records of the simultaneous observation at two stations, Ōfunato and Enoshima, by Tukey's method.

12) R. TAKAHASI, I. AIDA and Y. NAGATA, "The Submerged Long-wave Recorders and the Observation of the Seiches in Ōfunato Bay," *Jour. Oceanogr. Soc. Japan*, **22** (1966), 7, (in Japanese).

mostly identical, especially both characters being the same with respect to the phase response. Therefore, the corrections of the recorder characteristics for the calculated results were not made. In the figure, the coherence takes a low value in the whole range of frequency, but in both sides of 1 cycle per hour, their coherence becomes rather high. In the frequency bands showing the high coherence, both of the power-spectra at Enoshima and Ōfunato show certain peaks, the co-spectrum and quadrature-spectrum taking values of the same order, especially in 1.2 cycle per hour are they equal with each other. The phase curve shows that the record at Ōfunato delays from the one at Enoshima. The curves *a* and *b* on the phase diagram express the delay angles between Enoshima and Ōfunato expected from the calculation as mentioned in the preceding chapter. The coincidence of the theory and the observation for phase relation is not good. This may be due to a defect in the present analysis. The trapped mode and leaky mode are not separated, it being assumed that the whole of the disturbance is due to the trapped mode only. The results in the two cases mentioned above might be too poor to assert the existence of trapped waves in the back-ground fluctuations. However, the results shown in Figs. 10 and 11 will give us the necessary encouragement to continue the study on this problem.

#### 4. Conclusion

The trapped and leaky modes of oscillations on the shelf in the vicinity of Miyagi-Enoshima were calculated following the method presented by Munk et al. The results of the calculation based on one-dimensional approximation, taking the effect of Onagawa bay into account, show a good coincidence with the averaged spectrum at Enoshima of the water level fluctuations at ordinary time during a year in 1965. In the long period part of the spectrum, an attempt to confirm the existence of the trapped waves was tried, the results being insufficient to suggest the possible existence of such a wave. Therefore, to solve the problem, it is desired for the next step of the study that the water level fluctuations be observed simultaneously at several stations or more on the shelf.

#### 5. Acknowledgement

The author wishes to express his sincere thanks to Professor K.

Kajiura for his helpful advice, to Professor Y. Satô who allowed him to use the program of the Fourier analysis and to Dr. T. Momoi who also allowed him to use a sub-routine program. His thanks is also due to Mr. M. Koyama who has assisted him in reading out many records.

All the computations were made by utilizing the computer center of the University of Tokyo.

Finally, the author wishes to acknowledge his appreciation for the subsidy given to him from the Nomura Foundation, which was used as a part of the expenses in the present study.

### Appendix

Let  $x$  be drawn seaward, and  $y$  along the coastline pointing north.  $\zeta$  is the water rise above the undisturbed surface and  $c$  the long wave velocity. Then, the wave equation for constant depth is

$$\frac{\partial^2 \zeta}{\partial t^2} - c^2 \nabla^2 \zeta = 0. \quad (1)$$

The absorption due to viscosity is neglected. If the component travelling parallel to the shore is put to be

$$\zeta = \eta(x) \exp 2\pi i(ny - ft), \quad (2)$$

the wave profile normal to shore,  $\eta(x)$  is determined by

$$\frac{d^2 \eta}{dx^2} + \beta^2 \eta = 0, \quad \beta^2 = 4\pi^2 \left( \frac{f^2}{c^2} - n^2 \right), \quad (3)$$

with the solution

$$\left. \begin{aligned} \eta &= K_1 \cos \beta x + K_2 \sin \beta x & (\beta^2 > 0), \\ \eta &= K_1 + K_2 x & (\beta^2 = 0), \\ \eta &= K_1 \cosh |\beta| x + K_2 \sinh |\beta| x & (\beta^2 < 0), \end{aligned} \right\} \quad (4)$$

where  $n$  and  $f$  are spatial and time frequency respectively and  $K_1$  and  $K_2$  the integrating constant. The boundary condition at the coastline ( $x=0$ ) is that the flow normal to shore must vanish, the amplitude being given as  $A$ . In the joint of each step, continuities of water level and mass flux are given.

Then, the following matrix equation,



$$\mathbf{M}_N(0) = \mathbf{B}_{N-1} \dots \mathbf{B}_2 \mathbf{B}_1 \mathbf{M}_1(0) = \mathbf{C} \mathbf{M}_1(0) \quad (5)$$

is concluded, where

$$\mathbf{M}_i(x) = \begin{bmatrix} \eta_i(x) \\ h_i \eta'_i(x) \end{bmatrix}, \quad (6)$$

$$\mathbf{B}_i = \begin{bmatrix} \cos \beta_i l_i & \sin \beta_i l_i / \beta_i h_i \\ -\beta_i h_i \sin \beta_i l_i & \cos \beta_i l_i \end{bmatrix}, \quad (\beta_i^2 > 0), \quad (7)$$

and  $h_i$  and  $l_i$  are the water depth and the length of the  $i$ th step respectively. The water level and flux over the last step can be obtained by multiplying successively the matrix  $\mathbf{B}_i$  determined by the equation (7) to the matrix  $\mathbf{M}_1(0)$  on the shore. Now, in order to calculate the trapped modes propagating parallel to the shore, put the wave amplitude over the last step as

$$\eta_N = a \exp(-|\beta_N|x),$$

then

$$h_N \eta'_N = -|\beta_N| h_N a \exp(-|\beta_N|x).$$

The equation (5) becomes

$$\begin{bmatrix} a \\ -|\beta_N| h_N a \end{bmatrix} = \mathbf{C} \begin{bmatrix} A \\ 0 \end{bmatrix}. \quad (8)$$

In order that a solution exists, the determinant,

$$\mathbf{C}_{21} + |\beta_N| h_N \mathbf{C}_{11} \quad (9)$$

must vanish. The determinant has the solutions only for  $\beta_N^2 < 0$ . The computations have been carried out by the following program using a digital computer. The program evaluates  $\mathbf{C}$  and the determinant (9) for trial values of  $f$  and converges upon the eigensolutions by an iterative scheme.

As for the leaky modes, the wave amplitude over the last step is put to be

$$\eta_N = a \cos(\beta_N x + \alpha).$$

Then,

$$\begin{bmatrix} a \cos \alpha \\ -\beta_N h_N a \sin \alpha \end{bmatrix} = \mathbf{C} \begin{bmatrix} A \\ 0 \end{bmatrix}, \quad (10)$$

therefore, the squared ratio of coastal over incident amplitude is obtained by

$$R(f, n) = \frac{A^2}{a^2} = \frac{\beta_N^2 h_N^2}{\beta_N^2 h_N^2 C_{11}^2 + C_{21}^2} \quad (11)$$

The computations have been carried out in regard to the values of  $n$  and  $f$  with a proper interval in the domain  $\beta_N^2 > 0$ .

## 6. 宮城江の島附近の陸棚における海水振動

地震研究所 相 田 勇

陸棚上で観測された津波のスペクトルは、特別な擾乱源のない平常時の海面振動、所謂 back ground のスペクトルと密接な関係がある。それ故ここでは、この back ground の海面振動について、計算と実記録の解析の両面より考察を行った。

計算にあたっては、実際の陸棚のプロファイルを、30ケの階段状の形で近似して、Munk などによってなされた方法に従って、Trapped mode と Leaky mode の両方を求めた。又陸棚に女川湾が連なっている影響を考慮し、一次元の問題として、波が陸棚に直角に入射する場合に期待される、江の島、女川湾口、女川湾奥各点の海面振動のスペクトルを計算した。

一方、江の島津波観測所の長波計記録の1965年1年間から、擾乱の少ない日、24時間の長さの記録、24ケを抽出して、それぞれをフーリエ解析し、それらの一年間の平均スペクトル及び、季節毎の平均スペクトルを求めた。この観測記録のスペクトルは、季節的に殆んど変わらず、又先に計算された、女川湾の影響を考慮した場合の、江の島における海面振動スペクトルと極めてよく一致した。

観測スペクトルは、約50分より長周期の部分で、そのスペクトル振幅が増大する。これは、棚振動を誘発するエネルギーそのもののスペクトル構造によるものか、あるいは、Trapped mode の寄与によるものと考えられる。ここでは後者について吟味してみた。

即ち、観測記録のフーリエ解析によって得られている各周波数成分の位相と、陸棚上のある距離離れた一点から Trapped wave が伝播して来ると考えた場合に計算から期待される周波数に対する位相変化とを比較した。これによると、24ケのスペクトルの中、かなりよく一致するものが認められ、back ground の海面振動に Trapped wave が寄与しているという可能性を示している。又僅か一例であるが、江の島及び大船渡の2点同時観測のデータを用いて、Tukey の方法によって相関を求めた結果によると、Trapped wave の存在については明瞭ではない。